



ELSEVIER

Physics Letters B 544 (2002) 89–96

PHYSICS LETTERS B

www.elsevier.com/locate/npe

New measurements of the $D^+ \rightarrow \bar{K}^{*0} \mu^+ \nu$ form factor ratios

FOCUS Collaboration ¹

J.M. Link ^a, M. Reyes ^a, P.M. Yager ^a, J.C. Anjos ^b, I. Bediaga ^b, C. Göbel ^b, J. Magnin ^b,
 A. Massafferri ^b, J.M. de Miranda ^b, I.M. Pepe ^b, A.C. dos Reis ^b, S. Carrillo ^c,
 E. Casimiro ^c, E. Cuautle ^c, A. Sánchez-Hernández ^c, C. Uribe ^c, F. Vázquez ^c,
 L. Agostino ^d, L. Cinquini ^d, J.P. Cumalat ^d, B. O'Reilly ^d, J.E. Ramirez ^d, I. Segoni ^d,
 J.N. Butler ^e, H.W.K. Cheung ^e, G. Chiodini ^e, I. Gaines ^e, P.H. Garbincius ^e,
 L.A. Garren ^e, E. Gottschalk ^e, P.H. Kasper ^e, A.E. Kreymer ^e, R. Kutschke ^e,
 L. Benussi ^f, S. Bianco ^f, F.L. Fabbri ^f, A. Zallo ^f, C. Cawfield ^g, D.Y. Kim ^g, K.S. Park ^g,
 A. Rahimi ^g, J. Wiss ^g, R. Gardner ^h, A. Kryemadhi ^h, K.H. Chang ⁱ, Y.S. Chung ⁱ,
 J.S. Kang ⁱ, B.R. Ko ⁱ, J.W. Kwak ⁱ, K.B. Lee ⁱ, K. Cho ^j, H. Park ^j, G. Alimonti ^k,
 S. Barberis ^k, A. Cerutti ^k, M. Boschini ^k, P. D'Angelo ^k, M. DiCorato ^k, P. Dini ^k,
 L. Edera ^k, S. Erba ^k, M. Giammarchi ^k, P. Inzani ^k, F. Leveraro ^k, S. Malvezzi ^k,
 D. Menasce ^k, M. Mezzadri ^k, L. Moroni ^k, D. Pedrini ^k, C. Pontoglio ^k, F. Prelz ^k,
 M. Rovere ^k, S. Sala ^k, T.F. Davenport III ^l, V. Arena ^m, G. Boca ^m, G. Bonomi ^m,
 G. Gianini ^m, G. Liguori ^m, M.M. Merlo ^m, D. Pantea ^m, S.P. Ratti ^m, C. Riccardi ^m,
 P. Vitulo ^m, H. Hernandez ⁿ, A.M. Lopez ⁿ, H. Mendez ⁿ, A. Paris ⁿ, J. Quinones ⁿ,
 W. Xiong ⁿ, Y. Zhang ⁿ, J.R. Wilson ^o, T. Handler ^p, R. Mitchell ^p, D. Engh ^q,
 M. Hosack ^q, W.E. Johns ^q, M. Nehring ^q, P.D. Sheldon ^q, K. Stenson ^q,
 E.W. Vaandering ^q, M. Webster ^q, M. Sheaff ^r

^a University of California, Davis, CA 95616, USA

^b Centro Brasileiro de Pesquisas Físicas, Rio de Janeiro, RJ, Brazil

^c CINVESTAV, 07000 México City, DF, Mexico

^d University of Colorado, Boulder, CO 80309, USA

^e Fermi National Accelerator Laboratory, Batavia, IL 60510, USA

^f Laboratori Nazionali di Frascati dell'INFN, Frascati, I-00044 Italy

^g University of Illinois, Urbana-Champaign, IL 61801, USA

^h Indiana University, Bloomington, IN 47405, USA

ⁱ Korea University, Seoul, 136-701 South Korea

^j Kyungpook National University, Taegu, 702-701 South Korea

^k INFN and University of Milano, Milano, Italy

^l University of North Carolina, Asheville, NC 28804, USA

^m Dipartimento di Fisica Nucleare e Teorica and INFN, Pavia, Italy

ⁿ University of Puerto Rico, Mayaguez, PR 00681, Puerto Rico

^o University of South Carolina, Columbia, SC 29208, USA

^p University of Tennessee, Knoxville, TN 37996, USA

^q Vanderbilt University, Nashville, TN 37235, USA

^r University of Wisconsin, Madison, WI 53706, USA

Received 23 July 2002; accepted 25 July 2002

Editor: L. Montanet

Abstract

Using a large sample of $D^+ \rightarrow K^- \pi^+ \mu^+ \nu$ decays collected by the FOCUS photoproduction experiment at Fermilab, we present new measurements of two semileptonic form factor ratios: r_ν and r_2 . We find $r_\nu = 1.504 \pm 0.057 \pm 0.039$ and $r_2 = 0.875 \pm 0.049 \pm 0.064$. Our form factor results include the effects of the s -wave interference discussed in Phys. Lett. B 535 (2002) 43.

© 2002 Elsevier Science B.V. Open access under [CC BY](https://creativecommons.org/licenses/by/4.0/) license.

1. Introduction

This Letter provides new measurements of the parameters that describe $D^+ \rightarrow K^- \pi^+ \mu^+ \nu$ decay. In an earlier Letter [1] we described this process as the interference of a $D^+ \rightarrow \bar{K}^{*0} \mu^+ \nu$ amplitude with a constant s -wave amplitude. The $D^+ \rightarrow \bar{K}^{*0} \mu^+ \nu$ decay amplitude is described [2] by four form factors with an assumed (pole form) q^2 -dependence. Following earlier experimental work [3–8], the $D^+ \rightarrow \bar{K}^{*0} \mu^+ \nu$ amplitude is then described by ratios of form factors taken at $q^2 = 0$. The traditional set is: r_2, r_3 , and r_ν which we define explicitly after Eq. (1).

Five kinematic variables that uniquely describe $D^+ \rightarrow K^- \pi^+ \mu^+ \nu$ decay are illustrated in Fig. 1. These are the $K^- \pi^+$ invariant mass ($m_{K\pi}$), the square of the $\mu\nu$ mass (q^2), and three decay angles: the angle between the π and the D direction in the $K^- \pi^+$ rest frame (θ_ν), the angle between the ν and the D direction in the $\mu\nu$ rest frame (θ_ℓ), and the acoplanarity angle between the two decay planes (χ). These angular conventions on θ_ℓ and θ_ν apply to both the D^+ and D^- . The sense of the acoplanarity variable is defined via a cross product expression of the form: $(\vec{P}_\mu \times \vec{P}_\nu) \times (\vec{P}_K \times \vec{P}_\pi) \cdot \vec{P}_{K\pi}$, where all momentum vectors are in the D^+ rest frame. Since this expression involves five momentum vectors, as one goes from $D^+ \rightarrow D^-$ one must change $\chi \rightarrow -\chi$ in Eq. (1) to

get the same intensity for the D^+ and D^- assuming CP symmetry.

Using the notation of [2], we write the decay distribution for $D^+ \rightarrow K^- \pi^+ \mu^+ \nu$ in terms of the four helicity basis form factors: H_+, H_0, H_-, H_t .

$$\begin{aligned} & \frac{d^5 \Gamma}{dm_{K\pi} dq^2 d \cos \theta_\nu d \cos \theta_\ell d \chi} \\ & \propto K(q^2 - m_l^2) \\ & \times \left\{ |(1 + \cos \theta_\ell) \sin \theta_\nu e^{i\chi} B_{K^*0} H_+ \right. \\ & \quad - (1 - \cos \theta_\ell) \sin \theta_\nu e^{-i\chi} B_{K^*0} H_- \\ & \quad - 2 \sin \theta_\ell (\cos \theta_\nu B_{K^*0} + A e^{i\delta}) H_0|^2 \\ & \quad + \frac{m_\ell^2}{q^2} |\sin \theta_\ell \sin \theta_\nu B_{K^*0} (e^{i\chi} H_+ + e^{-i\chi} H_-) \\ & \quad + 2 \cos \theta_\ell (\cos \theta_\nu B_{K^*0} + A e^{i\delta}) H_0 \\ & \quad \left. + 2 (\cos \theta_\nu B_{K^*0} + A e^{i\delta}) H_t \right|^2, \end{aligned} \quad (1)$$

where K is the momentum of the $K^- \pi^+$ system in the rest frame of the D^+ . The first term gives the intensity for the μ^+ to be right-handed, while the (highly suppressed) second term gives the intensity for it to be left-handed. The helicity basis form factors are given by:

$$\begin{aligned} H_\pm(q^2) &= (M_D + m_{K\pi}) A_1(q^2) \\ & \mp 2 \frac{M_D K}{M_D + m_{K\pi}} V(q^2), \end{aligned}$$

¹ See <http://www-focus.fnal.gov/authors.html> for additional author information.

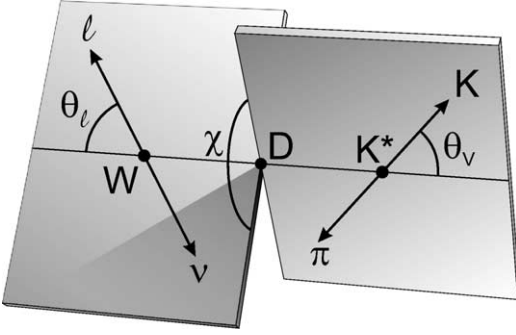


Fig. 1. Definition of kinematic variables.

$$\begin{aligned}
 H_0(q^2) &= \frac{1}{2m_{K\pi}\sqrt{q^2}} \\
 &\times \left[(M_D^2 - m_{K\pi}^2 - q^2)(M_D + m_{K\pi})A_1(q^2) \right. \\
 &\quad \left. - 4 \frac{M_D^2 K^2}{M_D + m_{K\pi}} A_2(q^2) \right], \\
 H_i(q^2) &= \frac{M_D K}{M_{K\pi}\sqrt{q^2}} \\
 &\times \left[(M_D + M_{K\pi})A_1(q^2) \right. \\
 &\quad \left. - \frac{(M_D^2 - M_{K\pi}^2 + q^2)}{M_D + M_{K\pi}} A_2(q^2) \right. \\
 &\quad \left. + \frac{2q^2}{M_D + M_{K\pi}} A_3(q^2) \right].
 \end{aligned}$$

The vector and axial form factors are generally parameterized by a pole dominance form:

$$A_i(q^2) = \frac{A_i(0)}{1 - q^2/M_A^2}, \quad V(q^2) = \frac{V(0)}{1 - q^2/M_V^2},$$

where we use nominal (spectroscopic) pole masses of $M_A = 2.5 \text{ GeV}/c^2$ and $M_V = 2.1 \text{ GeV}/c^2$.

² Eq. (1) implicitly assumes that the q^2 -dependence of the s -wave amplitude coupling to the virtual W^+ is the same as the H_0 form factor describing the $D^+ \rightarrow \bar{K}^{*0}\mu^+\nu$, but there is no theoretical justification for this assumption. This q^2 -dependence is compared to the data in Ref. [1]. We tried form factor ratio fits with an alternative, significantly different kinematic dependence for the s -wave amplitude where $H_0(q^2)$ is replaced by $K/(1 - q^2/M_A^2)$ in Eq. (1). We found that the values of r_2 and r_ν changed by less than 6% of their statistical error when fit with this alternative form.

The B_{K^*0} denotes the Breit-Wigner amplitude describing the \bar{K}^{*0} resonance:³

$$B_{K^*0} = \frac{\sqrt{m_0\Gamma}(P^*/P_0^*)}{m_{K\pi}^2 - m_0^2 + im_0\Gamma(P^*/P_0^*)^3}.$$

Under these assumptions, the decay intensity is then parameterized by the $r_\nu \equiv V(0)/A_1(0)$, $r_2 \equiv A_2(0)/A_1(0)$, $r_3 \equiv A_3(0)/A_1(0)$ form factor ratios describing the $D^+ \rightarrow \bar{K}^{*0}\mu^+\nu$ amplitude and the modulus A and phase δ describing the s -wave amplitude. Throughout this Letter, unless explicitly stated otherwise, the charge conjugate is also implied when a decay mode of a specific charge is stated.

2. Experimental and analysis details

The data for this Letter were collected in the Wideband photoproduction experiment FOCUS during the Fermilab 1996–1997 fixed-target run. In FOCUS, a forward multi-particle spectrometer is used to measure the interactions of high energy photons on a segmented BeO target. The FOCUS detector is a large aperture, fixed-target spectrometer with excellent vertexing and particle identification. Most of the FOCUS experiment and analysis techniques have been described previously [1,9–11]. Our analysis cuts were chosen to give reasonably uniform acceptance over the five kinematic decay variables, while maintaining a strong rejection of backgrounds. To suppress background from the re-interaction of particles in the target region which can mimic a decay vertex, we required that the charm secondary vertex was located at least one standard deviation outside of all solid material including our target and target microstrip system.

To isolate the $D^+ \rightarrow K^-\pi^+\mu^+\nu$ topology, we required that candidate muon, pion, and kaon tracks appeared in a secondary vertex with a confidence level exceeding 5%. The muon track, when extrapolated

³ We are using a p -wave Breit-Wigner form with a width proportional to the cube of the kaon momentum in the kaon-pion rest frame (P^*) over the value of this momentum when the kaon-pion mass equals the resonant mass (P_0^*). The squared modulus of our Breit-Wigner form will have an effective P^{*3} -dependence in the numerator as well. Two powers P^* come explicitly from the P^* in the numerator of the amplitude and one power arises from the 4-body phase space.

to the shielded muon arrays, was required to match muon hits with a confidence level exceeding 5%. The kaon was required to have a Čerenkov light pattern more consistent with that for a kaon than that for a pion by 1 unit of log likelihood, while the pion track was required to have a light pattern favoring the pion hypothesis over that for the kaon by 1 unit [11].

To further reduce muon misidentification, a muon candidate was allowed to have at most one missing hit in the 6 planes comprising our inner muon system and an energy exceeding 10 GeV. In order to suppress muons from pions and kaons decaying within our apparatus, we required that each muon candidate had a confidence level exceeding 2% to the hypothesis that it had a consistent trajectory through our two analysis magnets.

Non-charm and random combinatoric backgrounds were reduced by requiring both a detachment between the vertex containing the $K^- \pi^+ \mu^+$ and the primary production vertex of 10 standard deviations and a minimum visible energy ($E_K + E_\pi + E_\mu$) of 30 GeV. To suppress possible backgrounds from higher multiplicity charm decay, we isolate the $K\pi\mu$ vertex from other tracks in the event (not including tracks in the primary vertex) by requiring that the maximum confidence level for another track to form a vertex with the candidate be less than 0.1%.

In order to allow for the missing energy of the neutrino in this semileptonic D^+ decay, we required the reconstructed $K\pi\mu$ mass be less than the nominal D^+ mass. Background from $D^+ \rightarrow K^- \pi^+ \pi^+$, where a pion is misidentified as a muon, was reduced using a mass cut: we required when the muon track is treated as a pion and the combination is reconstructed as a $K\pi\pi$, the $K\pi\pi$ invariant mass differed from the nominal D^+ mass by at least three standard deviations. In order to suppress background from $D^{*+} \rightarrow D^0 \pi^+ \rightarrow (K^- \mu^+ \nu) \pi^+$ we required $M(K^- \mu^+ \nu \pi^+) - M(K^- \mu^+ \nu) > 0.18 \text{ GeV}/c^2$. The $m_{K\pi}$ distribution for our $D^+ \rightarrow K^- \pi^+ \mu^+ \nu$ candidates is shown in Fig. 2.

The technique used to reconstruct the neutrino momentum through the D^+ line-of-flight, and tests of our ability to simulate the resolution on kinematic variables that rely on the neutrino momentum are described in Ref. [1].

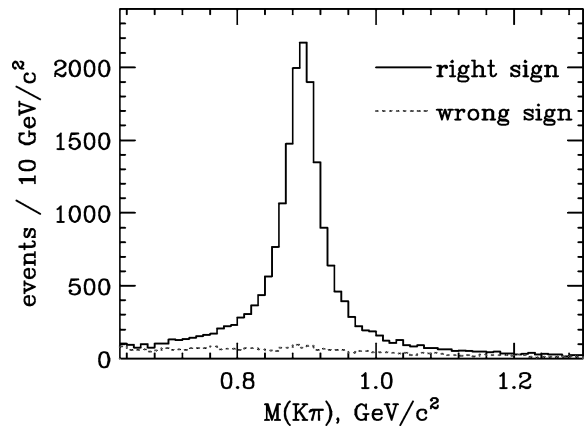


Fig. 2. $D^+ \rightarrow K^- \pi^+ \mu^+ \nu$ signal. Right-sign and wrong-sign samples are shown. In the mass window 0.8–1.0 GeV/c^2 there is a right-sign excess of 14 678 events. A Monte Carlo that simulates the production and decay of all known charm species predicts that $\approx 3\%$ of this excess is actually background from other charm decays.

3. Fitting technique

We use a binned version [12] of the fitting technique developed by the E691 Collaboration [13] for fitting decay intensities where some of the kinematic variables have very poor resolution such as the four variables that rely on reconstructed neutrino kinematics. The observed number of wrong-sign-subtracted events in each kinematic bin is compared to a prediction. The production is constructed from a $D^+ \rightarrow K^- \pi^+ \mu^+ \nu$ signal Monte Carlo incorporating s -wave interference [1] plus a wrong-sign-subtracted, charm background contribution predicted by a background Monte Carlo which simulates all known charm decays as well as our misidentification levels.

Although the charm background correction was fairly unimportant given the tight muon cuts used for our quoted results, this correction was important when looser muon cuts were employed. In the sample selected with looser muon cuts, the charm background increased from about 3% to 7% of the total right-sign excess. In fits to the looser sample, the charm background correction typically lowered the uncorrected r_ν by 0.15 (or about 2.7 times our statistical error) to a value very consistent with our quoted result. The charm background is primarily due to false muons from decays of pions and kaons in flight and therefore tends to populate low (lab) momentum or the negative $\cos\theta_\ell$ region. Including the

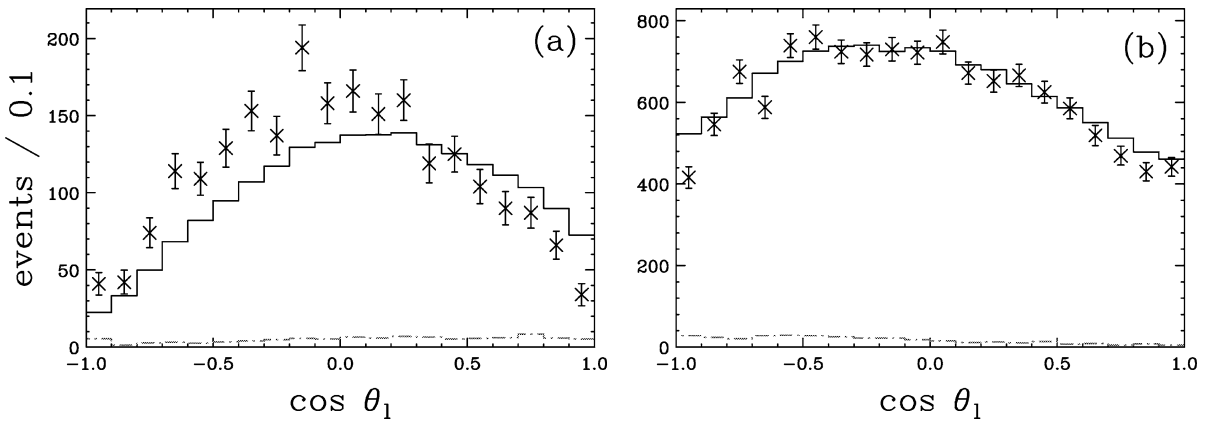


Fig. 3. We show the $\cos\theta_\ell$ distribution in two ranges for q^2 . The data are shown as points with error bars, while the Monte Carlo model which includes charm backgrounds are the solid line histograms. The predicted charm background contributions are the dashed lines. (a) shows events in the low q^2 region: $q^2 < 0.2 \text{ GeV}^2/c^2$. (b) shows events in the remaining q^2 region: $q^2 > 0.2 \text{ GeV}^2/c^2$.

background correction to the fit reduced the apparent backward-forward asymmetry in $\cos\theta_\ell$, thus reducing the difference between the H_+ and H_- form factor in Eq. (1). Since this difference is proportional to r_v , fits with the background correction will have a lower r_v relative to fits where no charm background correction was performed. The effect of charm backgrounds on the r_2 form factor ratio was found to be much smaller—about 1σ for our “loose” muon fits.

The signal Monte Carlo was initially generated flat in the $K\pi\mu\nu$ phase space and the five generated as well as reconstructed kinematic variables were stored for each event. The signal prediction for a given fit iteration is then computed by weighting each event within a given reconstructed kinematic bin by the intensity given by Eq. (1) evaluated using the five generated kinematic variables for the current set of fit parameters. The background Monte Carlo was normalized to the observed number of $D^+ \rightarrow K^-\pi^+\mu^+\nu$ events in the mass range $0.8 < m_{K\pi} < 1.0 \text{ GeV}/c^2$ after applying the wrong-sign subtraction. The signal Monte Carlo was normalized to the difference between the observed wrong-sign-subtracted yield and the predicted wrong-sign-subtracted background yield. The fit determined the physics parameters by minimizing the χ^2 over all bins.

Two fits were employed in this analysis: a fit to the s -wave amplitude with fixed r_v and r_2 form factor

ratios, and a fit to the r_v and r_2 form factors ratios⁴ with a fixed s -wave amplitude and phase. In the form factor fit, we used five bins in $\cos\theta_\nu$, five bins in $\cos\theta_\ell$, three bins in $|\chi|$, and three bins in q^2/q_{max}^2 for a total of 225 bins. This binning was chosen to be sensitive to the main features of our model intensity, Eq. (1), that depend on r_v and r_2 . The s -wave amplitude used three bins of $\cos\theta_\nu$, three bins of $\cos\theta_\ell$, four bins of $m_{K\pi}$, and three bins of χ for a total of 108 bins. The s -wave amplitude binning was chosen to emphasize the $m_{K\pi}$ dependence of the angular distribution. This dependence is extremely sensitive to the s -wave phase as discussed in Ref. [1]. In both cases, evenly spaced bins were used. The binnings of both fits were chosen to ensure at least 10 observed events per fit bin. These two fits were very loosely coupled so only a few iterations sufficed to obtain stable results.

Our initial form factor fits were of very poor quality due to a problem with our model matching the $\cos\theta_\ell$ distribution at very low q^2 ($q^2 < 0.2 \text{ GeV}^2/c^2$). Fig. 3 illustrates this problem by comparing the $\cos\theta_\ell$ distribution in data and our model for events below $q^2 = 0.2 \text{ GeV}^2/c^2$ and above $q^2 = 0.2 \text{ GeV}^2/c^2$, where the discrepancy is far less. Excluding the $q^2 < 0.2 \text{ GeV}^2/c^2$ region caused the χ^2 of our fits to

⁴ We decided not to fit for the r_3 form factor ratio since our anticipated r_3 error given our sample size and the q^2 cut described shortly would be ± 3 .

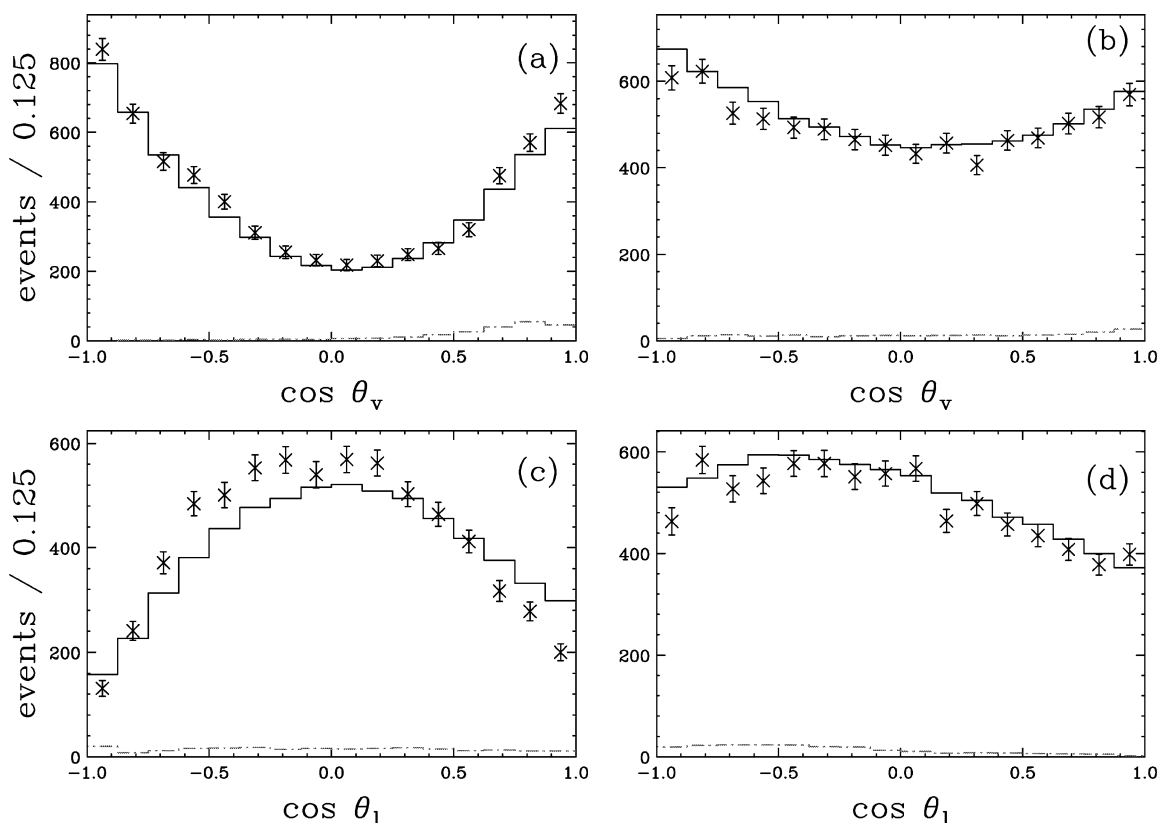


Fig. 4. Various $\cos\theta_v$ and $\cos\theta_\ell$ projections. The data are the points with error bars. The MC model predictions are the solid line histograms. The predicted charm background projections are the dashed lines. The model distributions are normalized by the total number of events in the sample rather than the area of each individual plot. (a) The $\cos\theta_v$ distribution for $q^2/q_{\max}^2 < 0.5$. (b) The $\cos\theta_v$ distribution for $q^2/q_{\max}^2 > 0.5$. (c) The $\cos\theta_\ell$ distribution for $q^2/q_{\max}^2 < 0.5$. (d) The $\cos\theta_\ell$ distribution for $q^2/q_{\max}^2 > 0.5$.

reduce by 86 units. The low q^2 discrepancy can most easily be explained as a deviation from the assumed pole dominance of the vector form factor, $V(q^2)$, but we have not eliminated all other possibilities. We have decided to exclude this region from our form factor and s -wave amplitude fits. When these regions were excluded, the fitted r_1 and r_2 form factor ratios decreased by 1.2σ and 0.4σ , respectively. With the $q^2 < 0.2 \text{ GeV}^2/c^2$ removed, our form factor fit has a χ^2 per degree of freedom of 1.15 for 223 degrees of freedom or a confidence level of 5.2%.

Figs. 4 and 5 compare the data and model for several of the more interesting projections of $\cos\theta_v$, $\cos\theta_\ell$, χ and q^2 . No q^2 cut is applied in these projections. Most of these distributions follow the predicted values reasonably well with the exception of

the low q^2 $\cos\theta_\ell$ projection (Fig. 4(c)) for the reasons discussed above.

The expected relative amounts of the $\cos\chi$ and $\cos 2\chi$ contributions and their phase variation as a function of $\cos\theta_v$ is well reproduced by our data as is the $\chi \leftrightarrow -\chi$ asymmetry created by the s -wave interference. The respective $\cos\theta_\ell > 0$ projections in data are also well matched by the model but show less variation than the acoplanarity distributions shown in Fig. 5.

Our s -wave amplitude fit produced an amplitude modulus of $A = 0.330 \pm 0.022 \pm 0.015 \text{ GeV}^{-1}$ and a phase of $\delta = 0.68 \pm 0.07 \pm 0.05 \text{ rad}$. Our estimate of the s -wave systematic error was based on the sample variance over 35 fits run with different analysis cuts. We varied such cuts as the particle identification

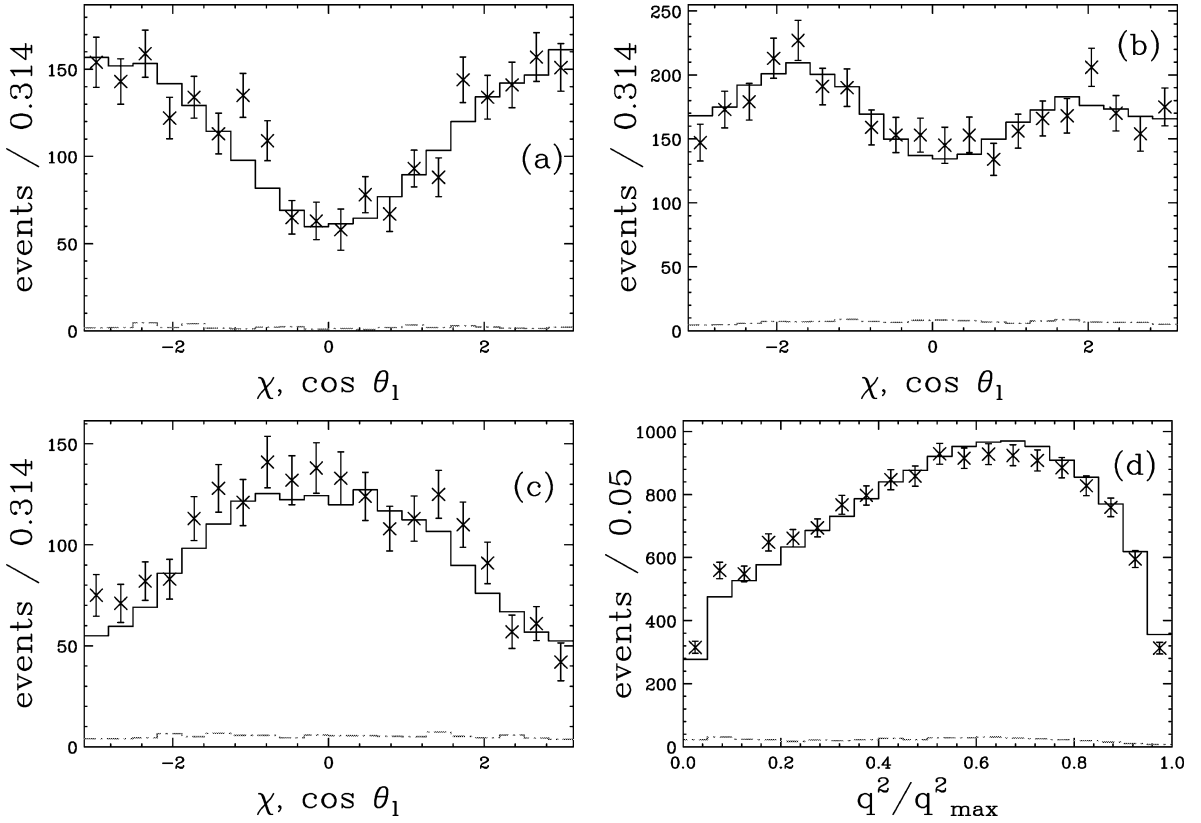


Fig. 5. Acoplanarity projections with $\cos\theta_\ell < 0$ and three ranges of $\cos\theta_v$. (a) $\cos\theta_v < -0.5$, (b) $-0.5 < \cos\theta_v < 0.5$ and (c) $0.5 < \cos\theta_v$. (d) The q^2/q_{\max}^2 projection. The data are the points with error bars. The models are the solid line histograms. The predicted charm backgrounds are the dashed lines.

cuts, vertexing cuts, and visible mass and energy cuts.

This result was then fed into our form factor fit to produce our r_v and r_2 measurements values.

A far more extensive systematic error analysis was made for the form factor analysis since these are actual physical parameters rather than an effective description of an interfering amplitude which is only validated in the vicinity of the \bar{K}^{*0} pole.

4. Form factor ratio systematic errors

Three basic approaches were used to determine the systematic error on the form factor ratios. In the first approach, we measured the stability of the branching ratio with respect to variations in analysis cuts designed to suppress backgrounds. In these studies we

varied cuts such as the detachment criteria, the secondary vertex quality, the minimal number of tracks in our primary vertex, particle identification cuts, visible momenta cuts, etc. Fifteen such cut sets were considered. In the second approach, we split our sample according to a variety of criteria deemed relevant to our acceptance, production, and decay models and estimated a systematic based on the consistency of the form factor ratio measurements among the split samples. We split our sample based on the visible D^+ momentum, particle versus antiparticle, and whether or not the $m_{K\pi}$ mass was above or below $0.9 \text{ GeV}/c^2$. This later split was based on our previous observation [1] of a large $\cos\theta_v$ asymmetry that developed for events with $m_{K\pi} < 0.9 \text{ GeV}/c^2$ due to the s -wave amplitude interference. In the third approach we checked the stability of the branching fraction as we varied specific parameters in our Monte Carlo model and fit-

Table 1
Measurements of the $D^+ \rightarrow \bar{K}^{*0} \ell^+ \nu_\ell$ form factor ratios

Group	r_v	r_2
This work	$1.504 \pm 0.057 \pm 0.039$	$0.875 \pm 0.049 \pm 0.064$
BEATRICE [3]	$1.45 \pm 0.23 \pm 0.07$	$1.00 \pm 0.15 \pm 0.03$
E791 (e) [4]	$1.90 \pm 0.11 \pm 0.09$	$0.71 \pm 0.08 \pm 0.09$
E791 (μ) [5]	$1.84 \pm 0.11 \pm 0.09$	$0.75 \pm 0.08 \pm 0.09$
E687 [6]	$1.74 \pm 0.27 \pm 0.28$	$0.78 \pm 0.18 \pm 0.11$
E653 [7]	$2.00 \pm 0.33 \pm 0.16$	$0.82 \pm 0.22 \pm 0.11$
E691 [8]	$2.0 \pm 0.6 \pm 0.3$	$0.0 \pm 0.5 \pm 0.2$

ting procedure. These included varying the level of the charm background Monte Carlo, and the value of the r_3 form factor ratio as a uniform variable over the range $-2 < r_3 < 2$.

Leaving out the s -wave amplitude contribution in our form factor fits *entirely* shifted both r_v and r_2 downward by only 0.5σ . Given the insensitivity of our form factor fits to the s -wave amplitude, no systematic error was assessed for uncertainty in the s -wave parameters. Combining all three non-zero systematic error estimates in quadrature we find $r_v = 1.504 \pm 0.057 \pm 0.039$ and $r_2 = 0.875 \pm 0.049 \pm 0.064$.

5. Summary

We presented a fit of the s -wave amplitude. We obtained an amplitude modulus of $A = 0.330 \pm 0.022 \pm 0.015 \text{ GeV}^{-1}$ and a phase of $\delta = 0.68 \pm 0.07 \pm 0.05 \text{ rad}$ in reasonable agreement with our very informal, previous [1] estimate of $A = 0.36 \times \exp(i\pi/4) \text{ GeV}^{-1}$. The inclusion of the s -wave amplitude dramatically improved the quality of our form factor fits but created only minor shifts in the resulting form factor ratio values.

Table 1 summarizes measurements of the r_v and r_2 form factor ratios. Our measurement is the first one to include the effects on the acceptance due to changes in the decay angular distribution brought about by the s -wave interference. We are consistent with the most recent previous measurement by the BEATRICE Collaboration. Our r_v value is about 2.9 standard deviations below the average of the two (previously most

precise) measurements by the E791 Collaboration although consistent with their value of r_2 .

Acknowledgements

We wish to acknowledge the assistance of the staffs of Fermi National Accelerator Laboratory, the INFN of Italy, and the physics departments of the collaborating institutions. This research was supported in part by the US National Science Foundation, the US Department of Energy, the Italian Istituto Nazionale di Fisica Nucleare and Ministero dell'Università e della Ricerca Scientifica e Tecnologica, the Brazilian Conselho Nacional de Desenvolvimento Científico e Tecnológico, CONACyT-México, the Korean Ministry of Education, and the Korean Science and Engineering Foundation.

References

- [1] FOCUS Collaboration, J.M. Link, et al., Phys. Lett. B 535 (2002) 43.
- [2] J.G. Korner, G.A. Schuler, Z. Phys. C 46 (1990) 93.
- [3] BEATRICE Collaboration, M. Adamovich, et al., Eur. Phys. J. C 6 (1999) 35.
- [4] E791 Collaboration, E.M. Aitala, et al., Phys. Rev. Lett. 80 (1998) 1393.
- [5] E791 Collaboration, E.M. Aitala, et al., Phys. Lett. B 440 (1998) 435.
- [6] E687 Collaboration, P.L. Frabetti, et al., Phys. Lett. B 307 (1993) 262.
- [7] E653 Collaboration, K. Kodama, et al., Phys. Lett. B 274 (1992) 246.
- [8] E691 Collaboration, J.C. Anjos, et al., Phys. Rev. Lett. 65 (1990) 2630.
- [9] E687 Collaboration, P.L. Frabetti, et al., Nucl. Instrum. Methods A 320 (1992) 519.
- [10] FOCUS Collaboration, J.M. Link, et al., Phys. Lett. B 485 (2000) 62.
- [11] FOCUS Collaboration, J.M. Link, et al., Nucl. Instrum. Methods A 484 (2002) 270.
- [12] E687 Collaboration, P.L. Frabetti, et al., Phys. Lett. B 364 (1995) 127.
- [13] D.M. Schmidt, R.J. Morrison, M.S. Witherell, Nucl. Instrum. Methods A 328 (1993) 547.